Channel Quality Estimation and Rate Adaptation for Cellular Mobile Radio

Krishna Balachandran, *Member, IEEE*, Srinivas R. Kadaba, *Member, IEEE*, and Sanjiv Nanda, *Member, IEEE*

***Abstract*—We propose a technique to measure channel quality in terms of signal-to-interference plus noise ratio (SINR) for the transmission of signals over fading channels. The Euclidean distance (ED) metric, associated with the decoded information sequence or a suitable modification thereof, is used as a channel quality measure. Simulations show that the filtered or averaged metric is a reliable channel quality measure which remains consistent across different coded modulation schemes and at different mobile speeds. The average scaled ED metric can be mapped to the SINR per symbol. We propose the use of this SINR estimate for data rate adaptation, in addition to mobile assisted handoff (MAHO) and power control. We particularly focus on data rate adaptation and propose a set of coded modulation schemes which utilize the SINR estimate to adapt between modulations, thus improving data throughput. Simulation results show that the proposed metric works well across the entire range of Dopplers to provide near-optimal rate adaptation to average SINR. This method of adaptation averages out short-term variations due to Rayleigh fading and adapts to the long-term effects such as shadowing. At low Dopplers, the metric can track Rayleigh fading and match the rate to a short-term average of the SINR, thus further increasing throughput.**

***Index Terms*— Adaptive modulation, channel quality estimation, Euclidean distance metric, rate adaptation.**

I. Introduction

ADAPTIVE data rate schemes using bandwidth efficient coded modulation are of interest for increasing throughput over channels with variable signal-to-interference plus noise ratio (SINR) due to fading, path loss, and interference such as those encountered in mobile radio. The information rate, transmitting at a fixed symbol rate, may be varied by changing the bandwidth efficiency (bits/symbol) using a choice of coded modulation schemes. For coded systems, the rate may be varied by i) fixing the modulation scheme and varying the code rate as in [1], ii) fixing the code rate and increasing the constellation size, or iii) a combination of i) and ii). In this paper we consider method ii), i.e., we fix the code rate and change the size of the constellation, thus increasing the data rate through the channel. At each SINR operating point, we wish to choose the coded modulation scheme which results in the highest throughput under retransmission delay constraints. Therefore, measurement of channel quality in terms of the SINR or achievable frame error rate is very important. Channel quality measurements are also essential for purposes of handoff and power control. Frame error rate measurements are usually very slow for the purpose of handoff, rate adaptation, or power control since observation over a large number of frames (equivalently, a large observation time interval) is necessary. Hence, there is a need for a reliable short-term (fast) channel quality indicator that can be related to the frame error rate. Adaptation can then be performed using a threshold based scheme.

Much of the earlier work can be broadly categorized into two classes. The first class primarily addresses estimation of channel quality, and the second addresses adaptive modulation techniques. We review these classes separately.

In the first class of work, channel quality metrics such as symbol error rate, bit error rate, and received signal strength measurements have been proposed as alternatives. However, measurement of the SINR has been the major point of interest in recent work. Austin and Stüber [2] investigated the performance of a training sequence based technique to estimate SINR; the accuracy of the technique depends on symbol error statistics if a training sequence is not used. Andersin *et al.* [3] proposed estimating the SINR using an eigendecomposition of the covariance matrix of the received signal. Türkboylari and Stüber [4] proposed another technique based on projecting the received signal onto a subspace representing the desired signal. The two latter techniques were shown to outperform the one in [2]. Recently, Jacobsmeyer [5] proposed the use of short-term increments of the Viterbi decoder metric computed over a sliding window as a channel quality indicator for fast rate adaption. Jacobsmeyer [5] also proposed the use of the difference between the incremental Viterbi decoder metrics for the best trellis path and the second best path as an alternative channel quality indicator for rate adaptation. A search for the second best path, however, requires greater decoder complexity. The metrics of [5] provide short-term indication of SINR but do not provide a measure of average SINR or long-term frame error rate. As a result, they are sensitive to instantaneous variations in channel quality. This can lead to many false alarms and misses and therefore affect the performance of automatic repeat request (ARQ) schemes.

Some early work on adaptive modulation was done by Hayes [6] and Cavers [7]. Recent work includes [8]–[10], with [8] and [10] addressing adaptive coded modulation and [9] primarily considering uncoded modulation. The adaptive coded modulation schemes proposed by Goldsmith and Chua

Manuscript received October 2, 1998; revised March 26, 1999.

K. Balachandran and S. Nanda are with Bell Labs, Lucent Technologies, Holmdel, NJ 07733 USA (e-mail: krishnab@lucent.com; nanda@lucent.com).

S. R. Kadaba is with Bell Labs, Lucent Technologies, Whippany, NJ 07981 USA (e-mail: skadaba@lucent.com).

Publisher Item Identifier S 0733-8716(99)06108-9.

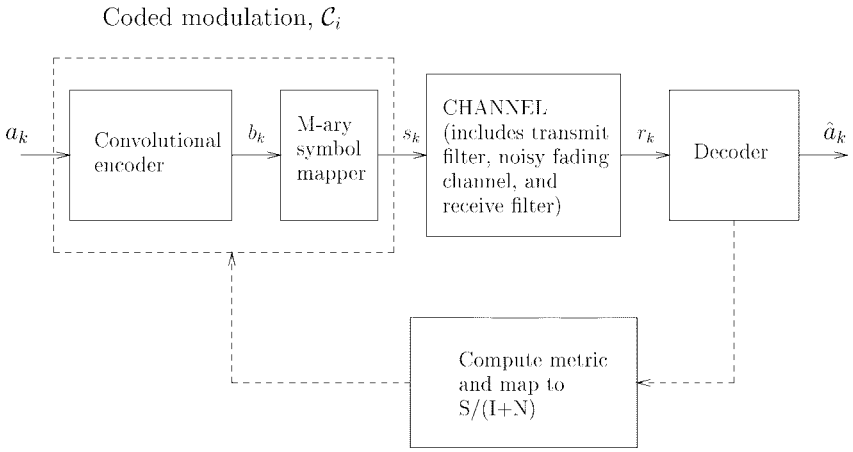

Fig. 1. Block diagram of system: equivalent baseband representation. Receiver provides channel quality feedback to the transmitter. a_k: information sequence; b_k: coded sequence; s_k: symbol sequence; r_k: received sequence; $\hat{a}_k$: decoded sequence.

[10] and Alamouti and Kallel [8] are conceptually similar. They consider a set of trellis coded modulation schemes and choose one based on the transmitter's knowledge of the SNR required to keep the bit error rate below a certain threshold. Assuming an ideal feedback channel that informs the transmitter about the channel SNR, the trellis code chooses symbols from a large set, thus achieving instantaneous adaptation. Symbol by symbol adaptation is difficult to achieve in practice due to feedback delay and feedback bandwidth constraints. In addition, such schemes result in high dynamic range signals, thus driving power amplifiers to inefficient operating points. On the other hand, such techniques provide valuable information in the form of achievable upper bounds.

The paper is organized as follows. Section II describes the system model and analysis for the channel quality metric. It concludes with a discussion on the applicability and use of the metric in various practical situations. Section III describes the rate adaptation methods considered, and addresses techniques for slow and fast feedback-based rate adaptation. The simulation conditions and the particular applications considered, i.e., the IS-136 channel extended to 8- and 16-level modulations, are described together in Section IV.A. The remainder of Section IV provides performance results. Other applications such as mobile assisted handoff (MAHO) and power control are briefly discussed in Section V, and conclusions are presented in Section VI.

II. Channel Quality Estimation

A. System and Channel Model

Consider the system schematic shown in Fig. 1. We assume frame by frame transmission, where there are K symbols transmitted in each frame. This is typical of all cellular systems. The information sequence $\{a_k\}$ is encoded using a convolutional encoder to provide a sequence $\{b_k\}$. The coded sequence $\{b_k\}$ is mapped into a symbol sequence $\{s_k\}$ from an M-ary constellation such as M-PSK (phase shift keying) or M-QAM (quadrature amplitude modulation) using either a Gray mapping or set-partitioning technique. In the first technique, the coded bit sequence $\{b_k\}$ is interleaved and Gray mapped into the constellation. This is referred to as bit-interleaved coded modulation (BICM) in the literature [11], [12]. Alternatively, the coded sequence $\{b_k\}$ may be mapped into the constellation using set-partitioning techniques and the resulting symbol sequence may be interleaved [13]. In either case, the code trellis is terminated in a known state every K symbols. Pulse shaping is carried out using transmit filters that satisfy the necessary and sufficient conditions for zero intersymbol interference. The signal is then transmitted over a wireless channel and is distorted by fading and additive white Gaussian noise (AWGN). The front end analog receive filter is assumed to be matched to the transmit filter, and its output is sampled at the optimal sampling instants. The received symbol at the kth time instant is then given by

$$r_k = \alpha_k s_k + \gamma_k i_k + n_k \tag{1}$$

where s_k denotes the transmitted symbol, α_k denotes the fading channel coefficient, i_k denotes the interfering symbol, γ_k denotes the interferer's fading coefficient, and n_k denotes the AWGN sample with variance N_o. All quantities are complex. The fading channel is assumed to be correlated and may be represented using the well-known Jakes model [14]. We assume that the receiver contains an automatic gain control (AGC) which maintains the long-term average of the signal power at unity. The effects of imperfect AGC are not considered in this paper. The state transitions of the convolutional encoder may be represented by a trellis, and decoding may be carried out using the Viterbi algorithm (VA).

Remark 1: In this paper, we assume the presence of a single dominant interferer (on the downlink), whose fading process is independent of that of the desired signal. A single dominant interferer represents the worst case scenario. If there are multiple interferers with nonnegligible power, the total interference appears closer to Gaussian. The Doppler bandwidth of the interferer's fading process is assumed to be the same as that of the desired signal since the Doppler bandwidth in the Rayleigh fading model is primarily dependent on the vehicle speed.

Remark 2: We are primarily concerned with the estimation of channel quality at the input to the decoder, so that the

discrete-time baseband channel (1) is the model of interest. The discrete-time baseband channel model assumes flat (or frequency nonselective) fading for both the signal and the interferer. The input to the decoder is the output of a matched filter and sampler, in the case of insignificant delay spread. If significant intersymbol interference (ISI) is caused due to larger delay spreads, then an equalizer with satisfactory performance would be employed to mitigate it. In this case, the input to the decoder would be the output of the equalizer and the discrete-time baseband channel is modified so that the noise term is augmented with the residual ISI, if any, after equalization.

B. Metrics for M-PSK

Notation: For a sequence $\{s_k\}$ of length K:

- $\{\tilde{s}_k\}$ denotes an arbitrary sequence of length K at the decoder;
- $\{\hat{s}_k\}$ denotes the estimate of $\{s_k\}$ at the decoder.

We assume that an estimate $\hat{\alpha}_k$ of the complex fading channel coefficient α_k is available at the kth instant to the decoder. Then, the Euclidean distance (ED) metric associated with a trellis path corresponding to an arbitrary sequence $\{\tilde{s}_k\}$ is given by

$$\Lambda_K^C(\{\tilde{s}_k\}) = \sum_{k=0}^{K-1} |r_k - \hat{\alpha}_k \tilde{s}_k|^2. \tag{2}$$

In the above, the superscript C denotes coherent detection (we will use D for differential detection). The Viterbi decoder chooses as the decoded sequence

$$\{\hat{s}_k\} = \arg\min_{\tilde{s}_k} \Lambda_K^C. \tag{3}$$

A good channel quality indicator metric should have the following properties: i) it should be independent of fading rates, i.e., the metric values should be consistent across a wide range of mobile speeds; ii) it should be independent of the size of the signal constellation in use; iii) it should be accurately estimable using a small number of samples; and iv) it should provide reliable indicators in both noise and interference limited conditions. In what follows, we propose deriving channel quality information from the cumulative ED metric Λ_K corresponding to the decoded trellis path for each block of length K. As we shall show later via simulation results, the ED metric possesses the desired properties and is readily available in any practical receiver. It thus proves to be an attractive candidate for our purposes. A small ED metric indicates that the received sequence is very close to the decoded sequence, which would occur at medium to high SINR values. Under poor SINR conditions, the metric is much larger. Therefore, the metric can be related to the SINR at the input to the demodulator/decoder. Indeed, from (1) and (2), the cumulative path metric corresponding to the decoded sequence $\{\hat{s}_k\}$ is given by

$$\Lambda_K^C(\{\hat{s}_k\}) = \sum_{k=0}^{K-1} |(\alpha_k s_k - \hat{\alpha}_k \hat{s}_k) + (\gamma_k i_k + n_k)|^2. \tag{4}$$

If perfect channel state information (CSI) is available, $\hat{\alpha}_k = \alpha_k$, and then (4) can be rewritten as

$$\Lambda_K^C(\{\hat{s}_k\}) = \sum_{k=0}^{K-1} |\alpha_k(s_k - \hat{s}_k) + (\gamma_k i_k + n_k)|^2. \tag{5}$$

The term $\alpha_k(s_k - \hat{s}_k)$ is equal to zero if the decoder does not make any errors. Typically, errors may occur when α_k is small but in such cases $\alpha_k(s_k - \hat{s}_k)$ is also small and may be neglected. Therefore

$$\frac{1}{K} E\left\{\sum_{k=0}^{K-1} |r_k - \alpha_k \hat{s}_k|^2\right\} \approx \frac{1}{K} E\left\{\sum_{k=0}^{K-1} |\gamma_k i_k + n_k|^2\right\} = (I + N) \tag{6}$$

where $E\{\cdot\}$ denotes expectation. Thus, the normalized expected value of the cumulative path metric may be considered as a close approximation to the interference plus noise power spectral density $(I + N)$ per symbol.

Following (4)–(6) above, we define the channel quality metric μ_K^C computed over K symbols as

$$\mu_K^C = \Lambda_K^C(\{\hat{s}_k\}). \tag{7}$$

Remark 3: Note that perfect CSI is not available in practice; however, CSI must be reliably estimated to achieve good error performance whenever coherent detection is employed. CSI can be reliably estimated in a number of ways, for example, using known pilot symbols inserted into the data sequence at regular intervals. The same estimate of CSI is used to compute the metric.

C. Metrics for M-DPSK

The computation in (2) assumes that the received signal is coherently demodulated and that an estimate of the channel coefficients is available to the receiver. A number of coded modulation schemes are designed using M-DPSK (differential phase-shift keying) constellations which allow a much simpler receiver structure [15]. These signals are often differentially detected prior to decoding, and no channel state information (CSI) is required for decoding. Here, at the kth instant, s_k denotes the differentially encoded complex transmitted symbol given by

$$s_k = d_k s_{k-1} \tag{8}$$

where d_k represents the complex PSK symbol generated by the symbol mapper.

The receiver first computes using differential detection and no CSI

$$y_k = r_k r_{k-1}^*. \tag{9}$$

The cumulative ED metric corresponding to a sequence $\{\tilde{d}_k\}$ is then given by

$$\Lambda_K^D(\{\tilde{d}_k\}) = \sum_{k=0}^{K-1} |y_k - \tilde{d}_k|^2. \tag{10}$$

Note that this metric does not use any CSI. The Viterbi decoder then chooses the sequence

$$\{\hat{d}_k\} = \arg\min_{\hat{d}_k} \Lambda_K^D. \tag{11}$$

There is an important difference between the decoder metrics for M-PSK and M-DPSK signaling. While the decoder metric also serves as a channel quality indicator for M-PSK, it does not do so for M-DPSK constellations. This is observed by analyzing the signal model (9) and the decoder metric (10). First, consider

$$\begin{aligned} y_k &= r_k r_{k-1}^* \\ &= (\alpha_k s_k + \gamma_k i_k + n_k)(\alpha_{k-1} s_{k-1} + \gamma_{k-1} i_{k-1} + n_{k-1})^*. \end{aligned} \tag{12}$$

Typically, the fading channel does not vary significantly from one symbol to the next, and so we get

$$y_k \approx |\alpha_k|^2 d_k + v_k \tag{13}$$

where $s_k s_{k-1}^* = d_k$, and we denote the sum of noise, interference, and cross terms by v_k. The ED metric corresponding to the decoded sequence $\{\hat{d}_k\}$ is now given by

$$\Lambda_K^D(\{\hat{d}_k\}) \approx \sum_{k=0}^{K-1} |(|\alpha_k|^2 d_k - \hat{d}_k) + v_k|^2. \tag{14}$$

For a correctly decoded frame, the metric can be expressed as

$$\Lambda_K^D(\{\hat{d}_k\}) \approx \sum_{k=0}^{K-1} |(|\alpha_k|^2 - 1) d_k + v_k|^2. \tag{15}$$

Unlike (5), in which the effect of the fading coefficient α_k vanishes, the metric (15) still depends upon α_k and, therefore, exhibits significant variability. This makes the metric strongly dependent upon the Doppler, which is undesirable. We now present a series of heuristic modifications to the channel quality metric for DPSK. In medium to high SINR, the signal component in (13) dominates, and since $|\alpha_k|^2$ is real, we can use $|y_k|$ to estimate it. First, the ED metric in (10) may be modified to obtain the ED metric with CSI

$$\begin{aligned} \Gamma_K &= \sum_{k=0}^{K-1} |y_k - |y_k| \hat{d}_k|^2 \\ &= \sum_{k=0}^{K-1} |(|\alpha_k|^2 - |y_k|) d_k + v_k|^2. \end{aligned} \tag{16}$$

Since $|y_k|$ closely approximates $|\alpha_k|^2$, the magnitude of the coefficient of d_k is very small in (16) above. The noise term, however, is still strongly dependent on the signal and its fading process. This can be seen by expanding the colored noise term

$$\begin{aligned} v_k = {} & \alpha_k s_k (\gamma_{k-1} i_{k-1} + n_{k-1})^* + \alpha_{k-1}^* s_{k-1}^* (\gamma_k i_k + n_k) \\ & + (\gamma_k i_k + n_k)(\gamma_{k-1}^* i_{k-1}^* + n_{k-1}^*). \end{aligned} \tag{17}$$

In medium to high SINR, the magnitudes of the first two terms dominate, and the magnitude of the last term is small. Then dividing by $\sqrt{|y_k|}$ (which is an estimate of $|\alpha_k|$) would mitigate the effect of the desired signal fading magnitude from the colored noise term. To this end, the metric can be refined to obtain the weighted ED metric with CSI

$$\Gamma'_K = \sum_{k=0}^{K-1} \frac{|y_k - |y_k| \hat{d}_k|^2}{|y_k|}. \tag{18}$$

At low Dopplers, the signal magnitude does not vary significantly over a frame, and hence $|y_k|$ in the denominator can be replaced by the received signal strength indicator (RSSI), which is given by $1/K \sum_{k=0}^{K-1} |r_k|^2$. Then, the scaled ED metric with CSI becomes

$$\Gamma''_K = \frac{\sum_{k=0}^{K-1} |y_k - |y_k| \hat{d}_k|^2}{\frac{1}{K} \sum_{k=0}^{K-1} |r_k|^2}. \tag{19}$$

Note that the RSSI can be obtained in real time at the sampler. Furthermore, (19) is easier to compute compared to (18) since it only requires one division operation. Simulation results indicated that the performance of both forms of the metric (18) and (19) were comparable across a wide range of Dopplers, i.e., the scaled ED metric with CSI (19) works well even at high Dopplers. Therefore, we set the channel quality metric, μ_K^D, equal to Γ''_K from (19) since it exhibits the desired properties and is easier to compute. We reiterate the fact that the channel quality metric (19) is different from the ED metric (10) used for decoding.

D. Observations

The channel quality metrics proposed above may be mapped to the SINR per symbol at the input to the decoder. We now describe the relationship between the channel quality metric and SINR and also discuss the impact of various system parameters and model assumptions on the proposed channel quality metrics.

1) Mapping to SINR: The long-term metric average μ can be mapped to the average SINR per symbol at the input to the decoder using

$$\widehat{\mathrm{SINR}}_{\mathrm{avg}} = 10 \log \frac{K}{\mu} \tag{20}$$

where $\widehat{\mathrm{SINR}}_{\mathrm{avg}}$ denotes the average SINR estimate, and μ denotes the average ED metric (in case of coherent detection) or the average normalized and scaled ED metric (in the case of DPSK with differential detection). In practice, a short-term running average of the metric may be used to predict the SINR. This approach enables quick tracking of the changes in channel conditions.

2) Decoder Implementation and Metric Computation: The advantage of the ED metric described above is that it can be decoupled from the decoding process. Although we chose a Viterbi decoder to decode the convolutional code at the receiver, this is not essential to the channel quality metric itself. For example, one may choose a maximum *a posteriori* (MAP) decoder or a reduced complexity sequential decoder for the convolutional code. Also, note that we have not assumed specific demodulation or equalization techniques prior to the decoder. Thus, the metric is independent of the specific receiver implementation. Using the decoded bits $\{\hat{a}_k\}$ as input to a local replica of the transmitter provides an estimate $\{\hat{s}_k\}$ of the transmitted symbol sequence. The channel quality metric

is now obtained by computing the ED metric or the normalized and scaled ED metric of the received symbol sequence from the locally generated estimate of the transmitted symbols. Therefore, the reliability of the metric depends only upon the quality of the decoder decisions.

3) Fading and Metric Averaging: The primary objective here is not to track short-term channel variations such as Rayleigh fading, but to track other long-term variations such as path loss and shadowing. In spite of this, the metric may display large variations from one block to another in the presence of fading. The long-term average of the ED metric smooths these variations out due to the averaging process, but the short-term metrics would still exhibit some variability. In such cases, smoothing or averaging of these variations is required to obtain a good estimate of the long-term metric. Simulation results presented later provide a more clear picture of the effects of metric averaging.

4) Interference and ISI: As mentioned earlier (see Remark 2), our signal model is applicable to the output of an equalizer, if one is used to mitigate ISI due to multipath and/or pulse shaping. In this case, the residual ISI is a signal dependent noise term. We expect that the proposed metrics would provide good SINR estimates even in the presence of residual ISI, especially when the equalizer is effective (i.e., at medium to high SINR). As shown above for DPSK, simple normalization and scaling can be used to mitigate the presence of signal dependent interference in the computation of the metric. We demonstrate the efficacy of such methods via simulations for the DPSK metric. The results show that signal dependent noise terms do not adversely affect the desirable properties of the channel quality metric.

III. Rate Adaptation

Current cellular systems are designed to achieve adequate coverage (SINR over a threshold) over most of the cell. As a result, a large portion of a typical cell has sufficient coverage to permit the use of coded modulation schemes with higher bandwidth efficiency. Let these schemes representing different modes of operation of the transmitter be denoted by $\mathcal{C}_1, \mathcal{C}_2, \ldots, \mathcal{C}_Q$ in ascending order of bandwidth efficiency. They may be implemented by using a fixed symbol rate and changing the trellis encoder and symbol mapper to pack a variable number of information bits per symbol.

We propose a threshold based adaptation scheme which switches between the coded modulation schemes depending upon the SINR. Let $\theta_1, \theta_2, \ldots, \theta_Q$ be SINR threshold values which are chosen such that between θ_{j-1} and θ_j, $j = 2, \ldots, Q-1$, the coded modulation scheme $\mathcal{C}_j$ has the highest throughput. Then, a transmitter mode (rate) adaptation scheme may be defined as follows:

Choose

$$\mathcal{C}_j \quad \text{if } \theta_{j-1} \le \frac{\hat{S}}{(I+N)} < \theta_j, \quad j = 2, \ldots, Q$$

else choose

$$\mathcal{C}_1 \quad \text{if } \frac{\hat{S}}{(I+N)} < \theta_1$$

else choose

$$\mathcal{C}_Q$$

where $\hat{S}/(I+N)$ denotes the estimated SINR.

Symbol by symbol adaptation is not assumed due to constraints in feedback delay and feedback bandwidth; instead, we define the adaptation interval T_a such that T_a is large enough to allow the transmission of at least one data frame and small enough to react quickly to changes in SINR. The transmitter may adapt its data rate every T_a s. The coded modulation schemes $\mathcal{C}_1, \mathcal{C}_2, \ldots, \mathcal{C}_Q$ may be chosen so that a variable integral number of frames are transmitted in time T_a, depending on the scheme. This allows efficient error recovery through ARQ mechanisms even with dynamic rate adaptation. The rate at which the transmitter reacts to changes in SINR depends on the measurement and feedback delay in the system. We consider both slow and fast feedback-based rate adaptation schemes and compute $\hat{S}/(I+N)$ for the threshold comparison according to the Doppler and the round trip delay.

A. Slow Feedback-Based Rate Adaptation

This technique is applicable at both low and high Dopplers. The transmitter does not react to short term or instantaneous variations in SINR, but adapts the data rate to changes in the average SINR. For the purpose of SINR threshold comparison, we set $\hat{S}/(I+N) = \widehat{\mathrm{SINR}}_{\mathrm{avg}}$ where $\widehat{\mathrm{SINR}}_{\mathrm{avg}}$ denotes the estimated average SINR. The average SINR is estimated using the channel quality metric. Short measurement averaging durations are sufficient since the receiver only tries to detect threshold crossings. Although smoothing is required for accurate estimation of SINR, threshold detection works well even without smoothing.

B. Fast Feedback-Based Rate Adaptation

At lower Dopplers, it may be possible to achieve higher throughputs by adapting the data rate to match the short-term (Rayleigh faded) SINR. A practical adaptation scheme which predicts the SINR at lower Dopplers and carries out faster rate adaptation is as follows. The SINR over the next adaptation interval may be predicted using

$$\mathrm{SINR}_{\mathrm{pred}} = \mathrm{RSSI}_{\mathrm{pred}}/\mu$$

where μ represents the short-term running average value of the channel quality metric. RSSI is predicted from past RSSI values which are computed using

$$\mathrm{RSSI} = \frac{1}{K}\sum_{k=0}^{K-1} |r_k|^2.$$

We use a simple RSSI predictor. Optimal prediction filters can be designed for further improvement in performance.

For SINR threshold comparison purposes, we set $\hat{S}/\,(I+N) = \mathrm{SINR}_{\mathrm{pred}}$ where $\mathrm{SINR}_{\mathrm{pred}}$ denotes the SINR predicted over the next adaptation interval. We also define two genie aided (ideal) adaptation schemes in which the errors due to measurement, prediction and feedback delay are eliminated. These schemes correspond to ideal rate adaptation for each

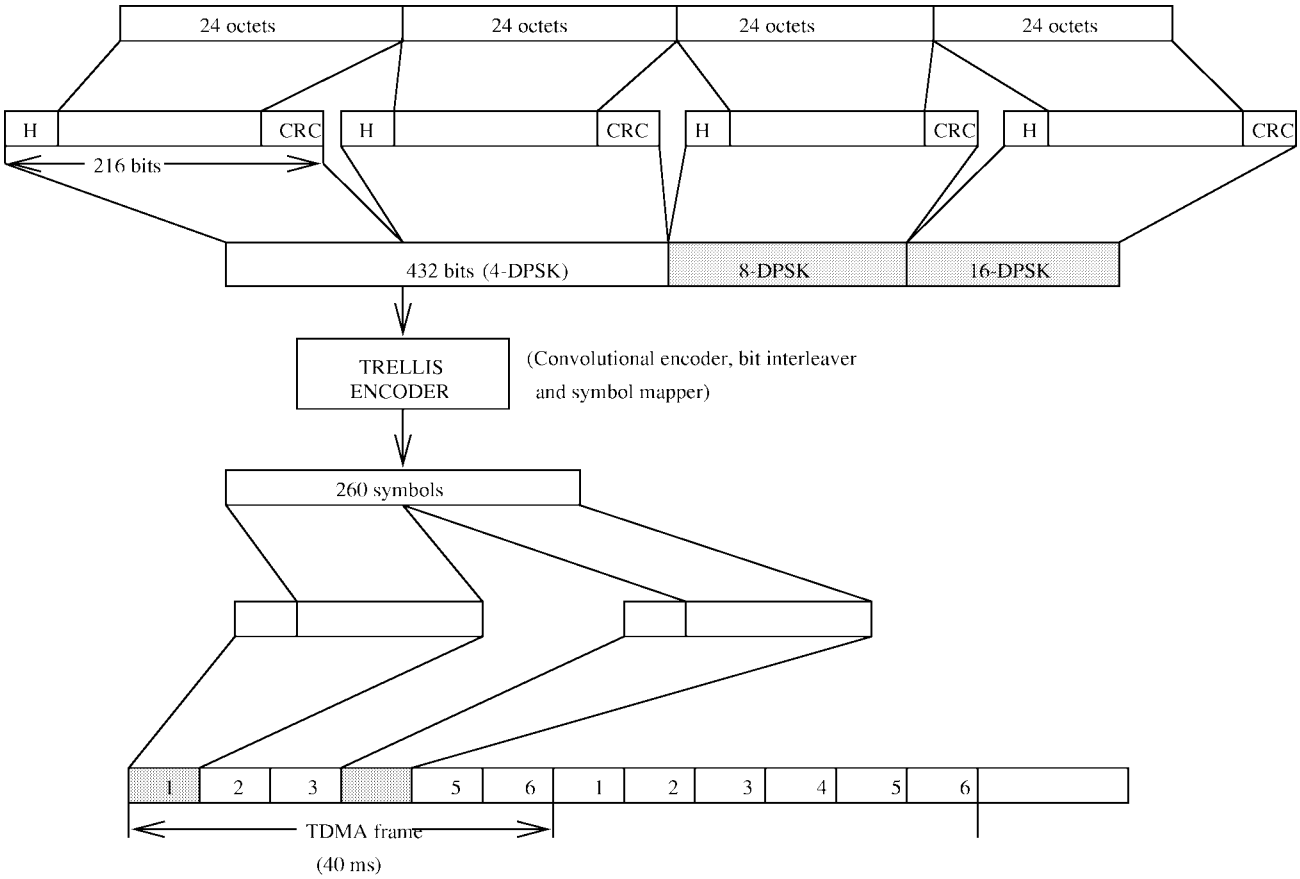

Fig. 2. Packing of multiple data frames into a time-slot pair.

adaptation interval and are theoretically interesting as upper bounds but unachievable in practice.

- *Known Decoder Outputs:* Choose the coded modulation scheme that gives the most good frames (hence maximizes throughput) for the next adaptation interval.
- *Known Channel SINR:* Choose the coded modulation scheme matched to the actual channel SINR for the next adaptation interval.

Simulation results showing the throughput performance achievable with slow and fast feedback-based rate adaptation are provided in the next section.

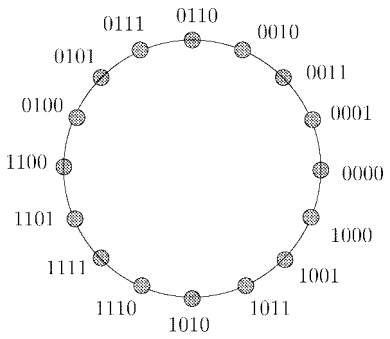

Fig. 3. Gray mapping for 16-PSK.

IV. Simulation Results

A. Simulation Assumptions

Simulations were carried out assuming the IS-136 North American Time Division Multiple Accesss (TDMA) downlink time-slot structure in which 260 symbols are transmitted interleaved over one time-slot pair (40 ms interval), as shown in Fig. 2. The information sequence is encoded using a rate 5/6, constraint length 6 (32 states) maximal free distance convolutional code punctured from a rate 1/2 code with octal generators, (53, 75). The outputs of the convolutional encoder are Gray mapped to 4-PSK, 8-PSK, or 16-PSK symbols. The Gray map for 16-PSK is shown in Fig. 3. The Gray maps for 4-PSK and 8-PSK are straightforward and not shown here. Alternatively, it is possible to use symbol interleaving in conjunction with set partition codes that are optimized for Rayleigh fading channels. Straightforward bit interleaved coding schemes were observed, however, to have frame error rate performance at least as good as asymptotically optimum set partition codes across the range of Doppler bandwidths and SINR values of interest.

For the rate adaptation simulations, the PSK symbol sequence, $\{d_k\}$, is differentially encoded using (8). We have fixed the code rate, but in general, the convolutional code and/or the modulation scheme may be changed to optimize throughput. Each data frame consists of 216 bits (8-bit header + 192 data bits data + 16-bit CRC), and two, three, or four frames may be transmitted per slot pair depending on whether 4-DPSK, 8-DPSK, or 16-DPSK, respectively, is used at the transmitter. This scheme of packing multiple data

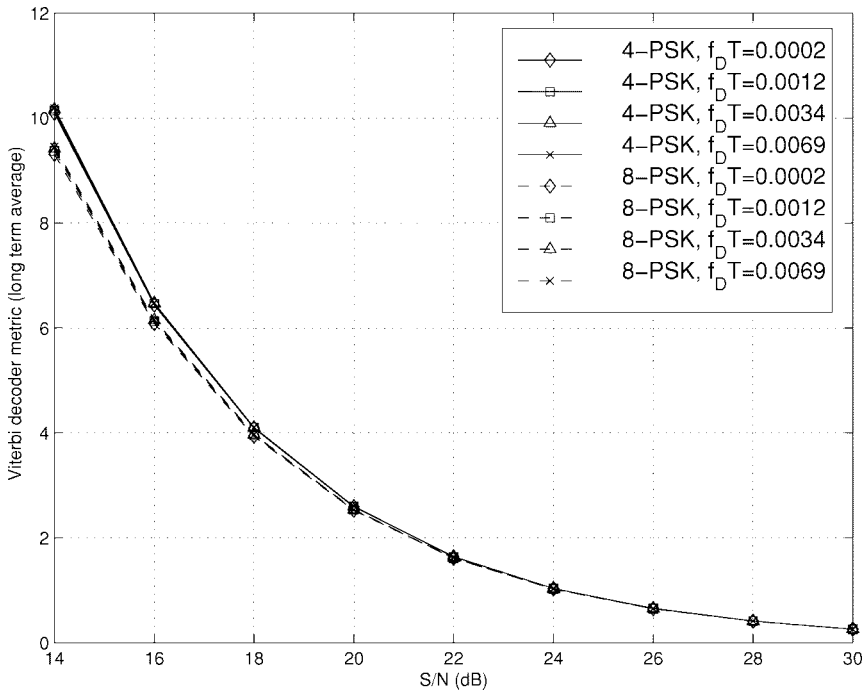

Fig. 4. Long-term average of Viterbi decoder metric versus S/N for rate 5/6 convolutionally coded coherent PSK (no interferers).

frames into a slot pair is shown in Fig. 2. The code trellis is terminated every time-slot pair.

We assume a flat Rayleigh fading channel model characterized by the product f_DT where f_D is the Doppler spread of the channel and T is the symbol time. The range of f_DT used in the simulations is from 0.0002 to 0.0069, which represents vehicle speeds between 5 km/h and 200 km/h at a carrier frequency of 900 MHz.

The simulations assume that the transmitter can switch the modulation with every time-slot pair based on the average SINR estimated by the receiver (i.e., the adaptation interval is assumed to be a time-slot pair). The observation interval is two time slots (26.67 ms), since coding and interleaving are carried out over a time-slot pair. At the end of each observation interval, an estimate of SINR is obtained. A further feedback (round-trip) delay of 93.33 ms is assumed. This includes the decoding delay and delay associated with modulation switching at the transmitter. Therefore, in the slow feedback case, the total delay is approximately 120 ms before the transmitter can react to changes in SINR.

For the fast feedback case, the simulation assumes RSSI feedback every 40 ms, in addition to the channel quality feedback every 120 ms. A third-order optimal one-step linear predictor is used for predicting the RSSI over the next time-slot pair from past RSSI values.

The switching thresholds θ_l and θ_h are chosen based on delay/throughput tradeoffs across the range of Dopplers. A 16-DPSK is used when the estimated SINR is larger than $\theta_h = 23$ dB, 8-DPSK is used when the estimated SINR lies between $\theta_l = 17$ dB and $\theta_h = 23$ dB, and 4-DPSK is used when the estimated SINR is less than $\theta_l = 17$ dB. Channel state information is not assumed to be known at either the transmitter or the receiver in the simulation. Rate adaptation is based solely on the metric and no averaging is applied to the normalized and scaled ED metric.

B. Long-Term Metric Average

We first examine the expected value (long-term average) of the proposed metrics. For the coherent case we had shown in (6) that the metric has the right expected value. We find from simulations that for DPSK the normalized and scaled ED metric (19) also has the "right" long-term average.

The channel quality metric for each block is computed using (4) for M-PSK assuming perfect CSI and (19) assuming differential detection and unknown CSI for M-DPSK. The results in Figs. 4 and 5 demonstrate that the averaged long-term metric μ, as a function of the SINR, is almost identical across the range of Dopplers and also across different modulations.

Interference limited conditions were simulated assuming that the fading process of the interferer is independent of that of the desired signal, but the Doppler bandwidths are the same. This is typical of the downlink. The long-term average of the metric for rate 5/6 convolutionally coded 4-DPSK in the presence of a similar interferer is shown in Fig. 6. We see that the metric still retains consistency across Dopplers.

We observe that the long-term average of the channel quality estimate shows negligible variability across Dopplers and is independent of the channel encoder, constellation density, and symbol mapping scheme under both noise limited and interference limited conditions. Recall that the metric computation may be decoupled from the decoding process. In this case, any suboptimum (reduced search) decoder may be used as long as the performance of the decoder is near maximum likelihood.

C. Metric Averaging Duration

The averaging duration determines the speed with which the estimator tracks changes in the actual SINR. The estimation

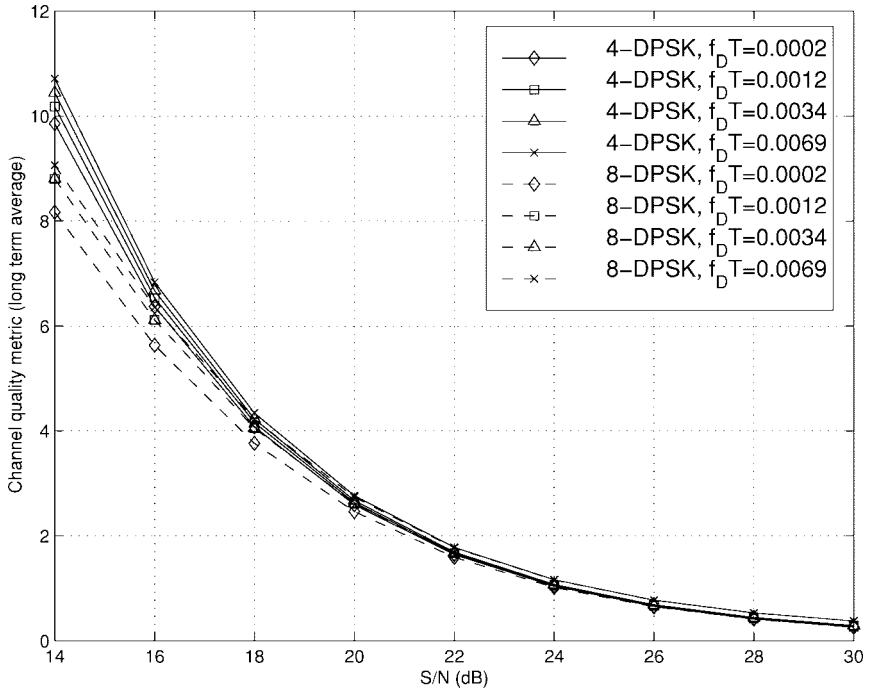

Fig. 5. Long-term average of scaled ED metric versus S/N for rate 5/6 convolutionally coded differential PSK (no interferers).

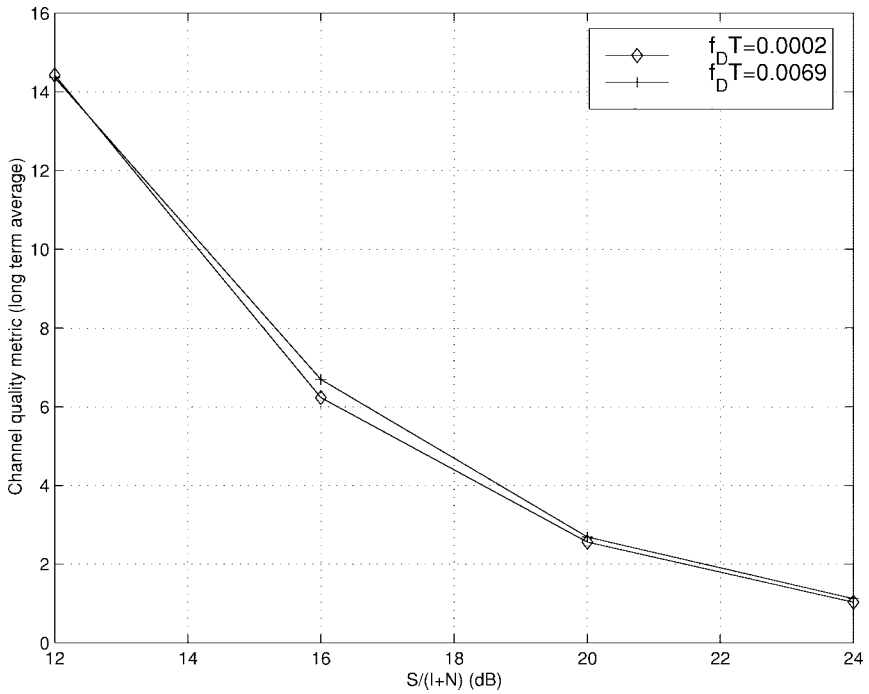

Fig. 6. Long-term average of scaled ED metric versus $S/(I+N)$ for rate 5/6 convolutionally coded 4-DPSK (differential detection, no CSI, $I/N = 20$ dB); the metric is consistent across Dopplers even with fading interferers.

error performance can be characterized, as in [2] and [4], by computing the average absolute error in the SINR estimate given by $E\{|\mathrm{SINR}_{\mathrm{estimated}}\ (\mathrm{dB}) - \mathrm{SINR}_{\mathrm{actual}}\ (\mathrm{dB})|\}$. Fig. 7 shows that under noise limited conditions (i.e., $I = 0$), the metric requires little or no averaging, and the absolute error in the SINR estimate is less than 0.25 dB at all Dopplers.

The estimation error for the interference limited case is shown in Fig. 8. Under these conditions, the absolute error in the SINR estimate is larger at lower Dopplers (approximately 2 dB with an averaging duration of 300 ms, but reducing to less than 1 dB at 900 ms). At larger Dopplers, however, the absolute estimation error is less than 0.5 dB with the same averaging durations.

The estimation error performance of the proposed technique is significantly better than the technique in [2] and comparable to the one in [4]. This implies that the averaged metric is suitable for applications like MAHO for which the earlier techniques were proposed. Moreover, the new metrics also

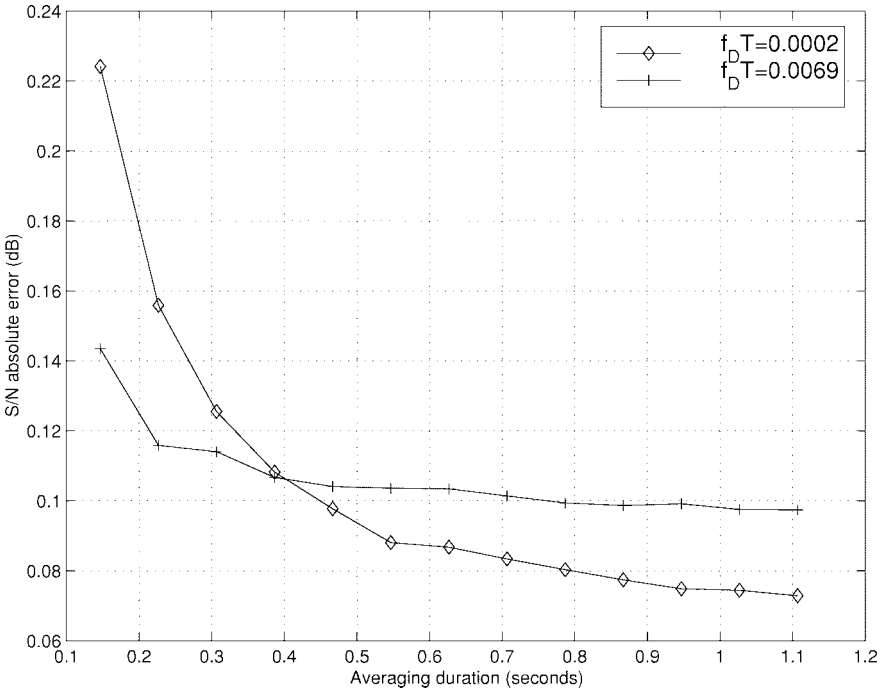

Fig. 7. S/N estimation error as a function of averaging duration for different Dopplers; rate 5/6 convolutionally coded 4-DPSK, $S/N = 16$ dB, differential detection, no CSI.

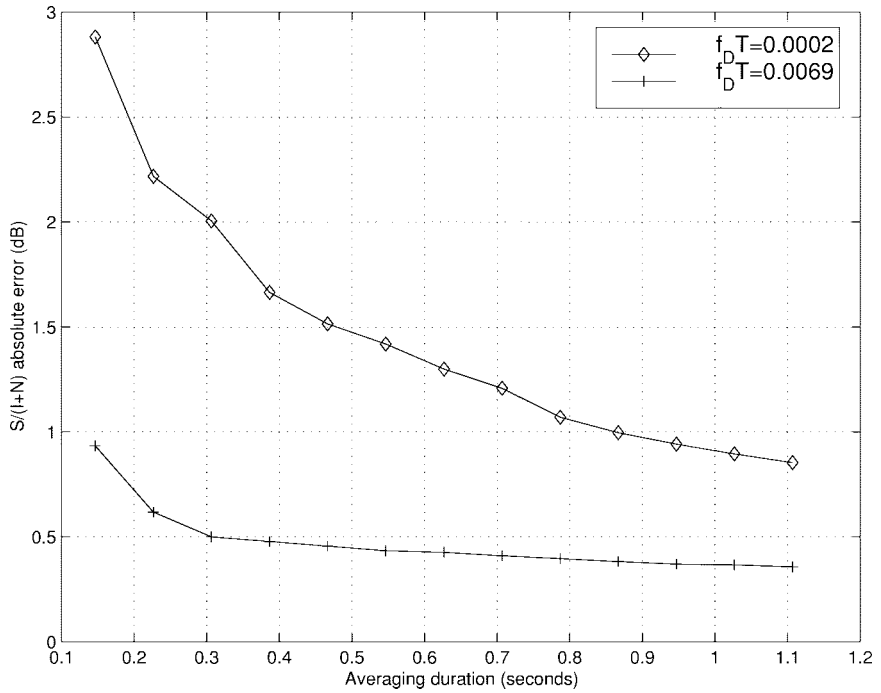

Fig. 8. $S/(I+N)$ estimation error as a function of averaging duration for different Dopplers; rate 5/6 convolutionally coded 4-DPSK, $S/(I+N) = 16$ dB, $I/N = 10$ dB, differential detection, no CSI.

account for nonideal receivers through residual errors at the decoder input. In the remainder of the paper, we examine the performance of the metric when used for rate adaptation.

D. Slow Feedback-Based Rate Adaptation

We first consider the noise limited case, i.e., $I = 0$. Rate adaptation is based on the scheme described in Table I. No averaging is used, that is, the normalized and scaled ED metric computed at the receiver for each time-slot pair is fed back to the transmitter and used to choose the modulation for the transmission in the time-slot pair with a delay of 120 ms.

The throughput performance of the adaptation scheme is shown in Figs. 9 and 10 for flat Rayleigh fading with $f_DT = 0.0002$ and $f_DT = 0.0069$, respectively. Results show that at higher Dopplers, the adaptation scheme chooses the coded

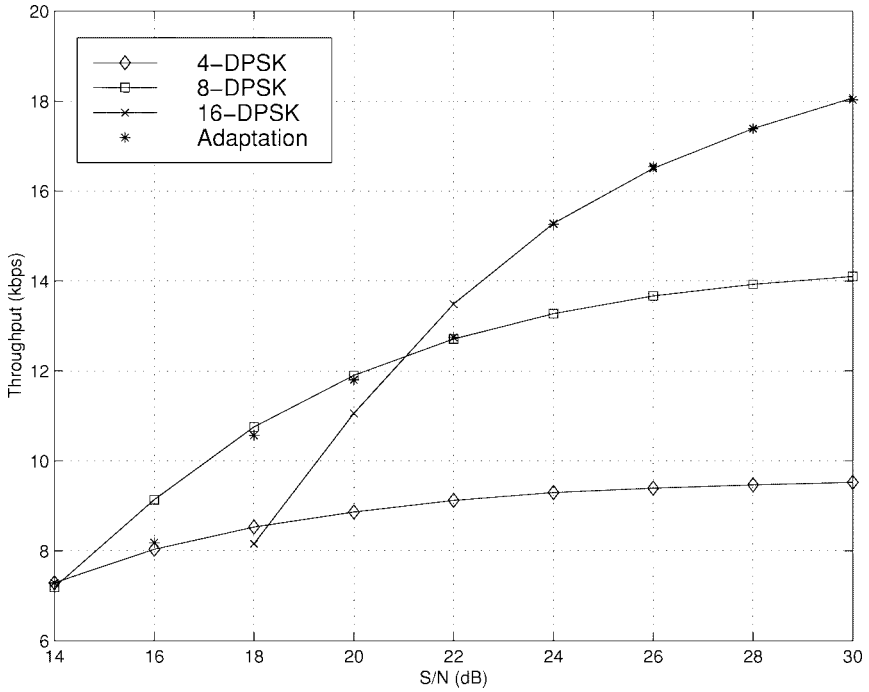

Fig. 9. Throughput for slow feedback-based rate adaptation in noise limited conditions; $f_D T = 0.0002$.

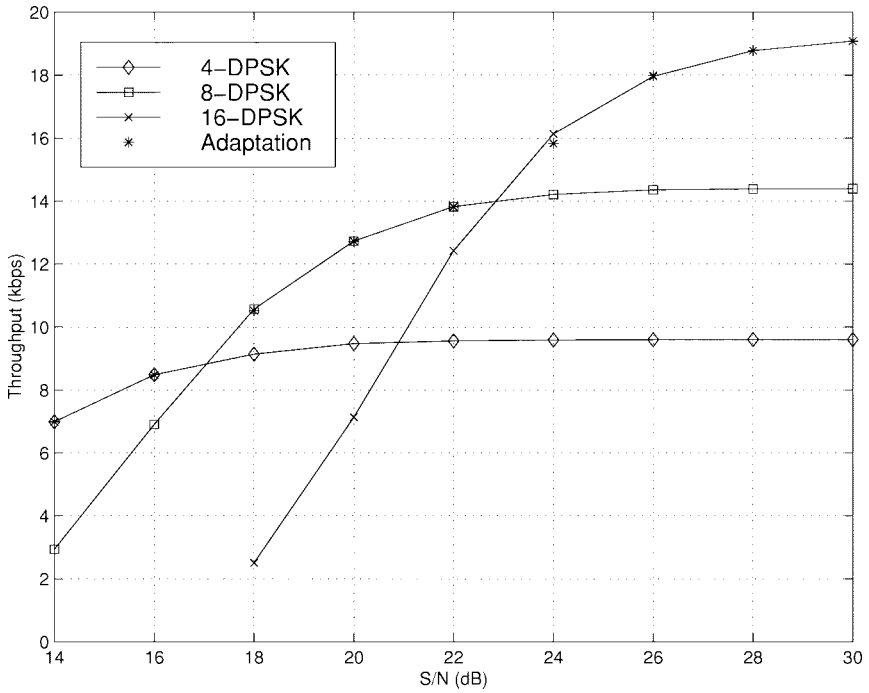

Fig. 10. Throughput for slow feedback-based rate adaptation in noise limited conditions; $f_D T = 0.0069$.

TABLE I
RATE ADAPTATION SCHEME BASED ON SINR USING A MODIFIED CUMULATIVE ED METRIC; θ_l AND θ_h DENOTE THRESHOLD VALUES

Conditions on estimated SINR	System mode	Bandwidth efficiency
$SINR < \theta_l = 17dB$	Coded 4-DPSK	1.67 bits/symbol
$\theta_l \leq SINR < \theta_h = 23dB$	Coded 8-DPSK	2.5 bits/symbol
$SINR \geq \theta_h$	Coded 16-DPSK	3.33 bits/symbol

modulation scheme which results in the highest throughput. Simulations have also shown that the performance of the adaptation scheme is relatively insensitive to delay.

Simulations were repeated for interference limited environments. A single downlink interferer was assumed; multiple interferers result in performance similar to the noise limited case and are not considered here. Fig. 11 shows the results assuming a flat Rayleigh fading channel with $f_D T = 0.0002$.

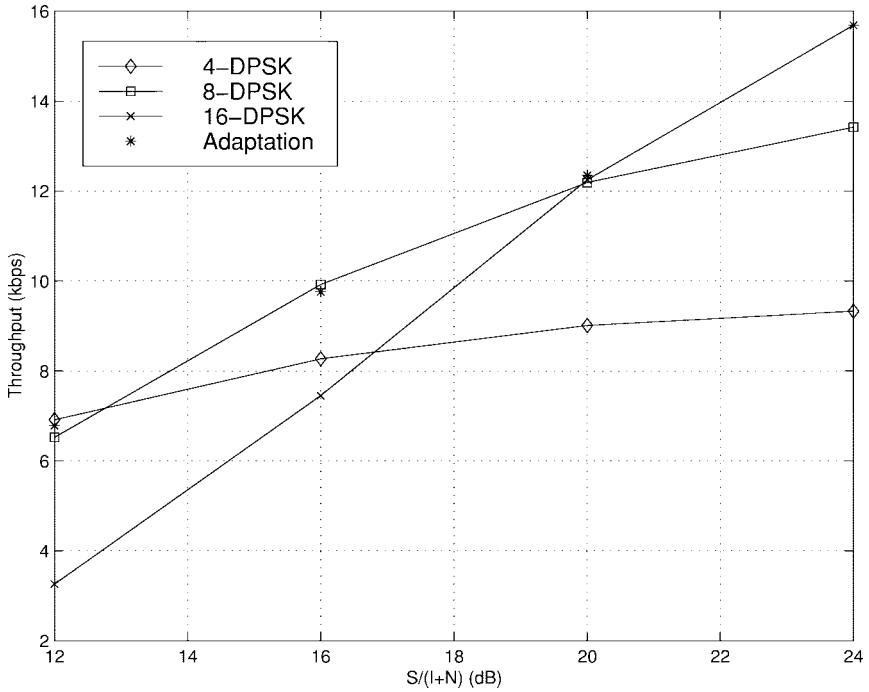

Fig. 11. Throughput for slow feedback-based rate adaptation in interference limited conditions; $f_D T = 0.0002$.

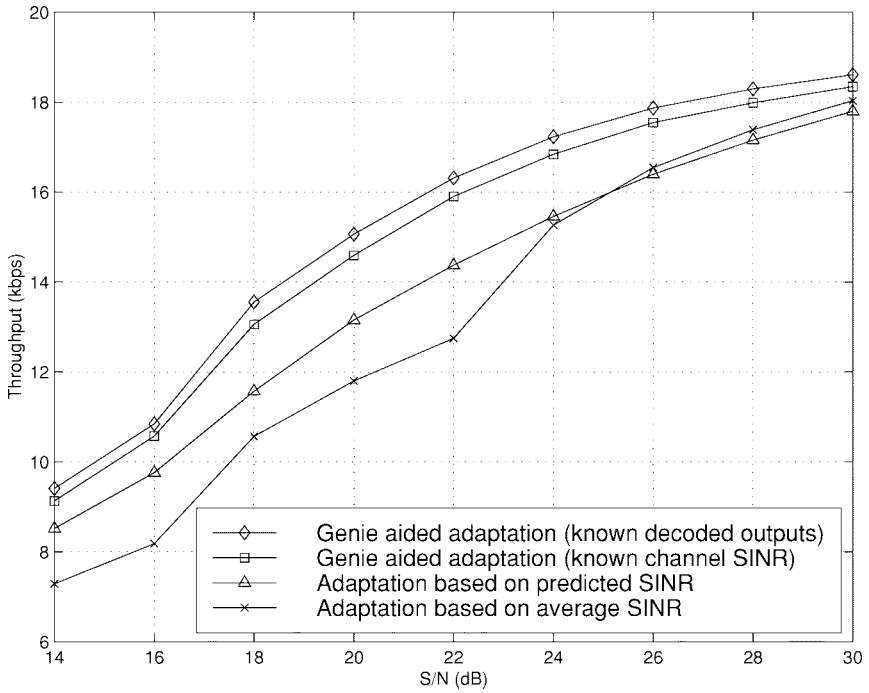

Fig. 12. Throughput achieved by different fast feedback-based adaptation strategies for $f_D T = 0.0002$.

Only the low Doppler case is considered here, since that represents the worst case in terms of SINR estimation performance with short averaging duration (see Fig. 6). Moreover, low mobility environments are of greater interest for data applications. The SINR thresholds were fixed at $\theta_l = 17$ dB and $\theta_h = 23$ dB. In both the noise limited and interference limited cases, the performance of the adaptation scheme may be improved at lower Dopplers by decreasing the thresholds. This, however, may cause some reduction in throughput at higher Dopplers. For example, in the noise limited case with $f_d T = 0.0069$, if the SINR thresholds are both lowered by 1 dB, the throughput reduces from approximately 13.8 kb/s to 12.5 kb/s at $\mathrm{SINR} = 22$ dB, and approximately 8.5 kb/s to 7 kb/s at $\mathrm{SINR} = 16$ dB (see Fig. 10).

E. Fast Feedback-Based Rate Adaptation

In the previous section we have shown results for rate adaptation based on using the average SINR estimate. At lower

Dopplers, it may be possible to achieve higher throughputs by adapting the rate to match the short-term (Rayleigh faded) SINR. Such rate adaptation to compensate for Rayleigh fadings is useful only at low Dopplers (f_D less than 10 Hz), since in the cellular TDMA context, achievable round trip feedback delays can be no shorter than 40–120 ms. In this section we study the improvements in throughput possible at low Dopplers through faster rate adaptation.

Fig. 12 shows the throughput achieved by the proposed fast feedback-based rate adaptation scheme for the noise limited case. We choose a low Doppler bandwidth $(f_D T = 0.0002)$. Also shown are the results for the average SINR based rate adaptation and the upper bounds to performance given by the two genie aided adaptation schemes described earlier. Fast feedback-based rate adaptation according to predicted SINR values achieves significant improvement in throughput, especially at low SINR. Further gains may be achievable with better prediction of SINR, as given by the upper bound for the genie-aided scheme where the channel SINR for the next slot pair is known.

At high Dopplers the situation is different. Slot-by-slot SINR prediction is harder, and the average SINR may be the best metric for rate adaptation. Moreover, as shown in Section IV-C (Figs. 7 and 8), at high Dopplers, we can obtain excellent estimates of average SINR with a short observation interval. Thus, under the slot-by-slot adaptation constraint, for fast fading conditions, rate adaptation based on the average SINR (as in the previous section) provides the best performance.

V. Other Applications

The proposed channel quality metrics can also be used for other applications such as MAHO and power control. We now briefly describe them.

A. Mobile Assisted Handoff (MAHO)

It is important for the mobile to accurately measure channel quality and report it to the serving base station, so that it can hand off before the performance becomes unacceptable leading to a dropped call. Measures such as received signal strength and symbol/bit error rates do not correlate well with the frame error rate (FER) which is widely accepted as the meaningful measure of performance in wireless systems. Also, received signal strength measurements are often coarse and inaccurate. The SINR is a more appropriate handoff metric near the cell boundary. The ED metric can be used as an implicit measure of the SINR to determine when handoff becomes necessary. The mobile terminal can use the ED metric to determine the SINR on the traffic channel, and report it to the base station. The base station then directs the mobile to handoff when the SINR reported by the mobile drops below a threshold.

B. Power Control

Power control is used in cellular mobile radio systems to combat path loss, fading, near-far situations and also to improve mobile terminal battery life. Again, in this case, the ED metric may be used as an implicit measure of SINR in order to provide feedback to the transmitter and control power levels.

VI. Conclusion

Adaptive data rate schemes which vary the coding and modulation schemes at the transmitter based on channel quality feedback from the receiver are very useful in achieving high throughputs in fading channels. We propose the use of the VA metric, or an appropriately chosen Euclidean distance metric, to obtain reliable channel quality information in terms of the average signal to interference plus noise ratio. For DPSK modulations, we propose a normalized and scaled Euclidean distance metric to provide reliable channel quality estimate. These channel quality metrics provide very good estimates of SINR for different (coherent and differential) coded modulation schemes across the range of Doppler bandwidths in both noise limited and interference limited environments. The metrics have the desirable attributes of being easily measurable in practical receivers and providing consistent estimates across a wide range of Dopplers and modulations. The proposed channel quality metric is found to provide robust estimates, even for the case of the weak rate 5/6 punctured convolutional code considered here.

A rate adaptation scheme which uses this metric to change the modulation at the transmitter has been described. Simulations show that this scheme achieves near optimal[1] throughputs under different conditions, and under reasonable feedback delay constraints. At lower Dopplers, it is possible to improve throughput by adapting to the instantaneous SINR, and achieve much closer performance to the ideal genie aided adaptation schemes described.

The proposed Euclidean distance metric can also be used to provide reliable channel quality information to facilitate mobile assisted handoff and power control schemes.

Acknowledgment

The authors gratefully acknowledge the contributions of three anonymous reviewers whose careful reviews have greatly improved the organization and clarity of the paper.

References

[1] J. Hagenauer, "Rate compatible punctured convolutional codes (RCPC codes) and their applications," *IEEE Trans. Commun.*, vol. 36, pp. 389–400, Apr. 1988.
[2] M. D. Austin and G. L. Stüber, "In service signal quality estimation for TDMA cellular systems," in *Proc. PIMRC*, 1995, pp. 836–840.
[3] M. Andersin, N. B. Mandayam, and R. D. Yates, "Subspace based estimation of the signal to interference ratio for TDMA cellular systems," in *Proc. VTC*, Atlanta, GA, 1996, pp. 1155–1159.
[4] M. Türkboylari and G. L. Stüber, "An efficient algorithm for estimating the signal-to-interference ratio in TDMA cellular systems," *IEEE Trans. Commun.*, vol. 46, pp. 728–731, June 1998.
[5] J. M. Jacobsmeyer, "Adaptive data rate modem," U.S. Patent 5 541 955, July 1996.
[6] J. F. Hayes, "Adaptive feedback communications," *IEEE Trans. Commun. Technol.*, vol. COM-16, pp. 29–34, Feb. 1968.
[7] J. K. Cavers, "Variable-rate transmission for Rayleigh fading channels," *IEEE Trans. Commun.*, vol. COM-20, pp. 15–22, Feb. 1972.
[8] S. M. Alamouti and S. Kallel, "Adaptive trellis-coded multiple-phase-shift keying for Rayleigh fading channels," *IEEE Trans. Commun.*, vol. 42, pp. 2305–2314, June 1994.

[1] Optimality is based on throughput as a function of average SINR.

[9] W. T. Webb and R. Steele, "Variable rate QAM for mobile radio," *IEEE Trans. Commun.*, vol. 43, pp. 2223–2230, July 1995.
[10] A. Goldsmith and S.-G. Chua, "Adaptive coded modulation for fading channels," *IEEE Trans. Commun.*, vol. 46, pp. 595–602, May 1998.
[11] E. Zehavi, "8-PSK trellis codes for a Rayleigh channel," *IEEE Trans. Commun.*, vol. 40, pp. 873–884, May 1992.
[12] G. Caire, G. Taricco, and E. Biglieri, "Bit-interleaved coded modulation," *IEEE Trans. Inform. Theory*, vol. 44, pp. 927–946, May 1998.
[13] G. Ungerboeck, "Channel coding with multi-level/phase signals," *IEEE Trans. Inform. Theory*, vol. IT-28, pp. 55–67, Jan. 1982.
[14] W. C. Jakes, *Microwave Mobile Communications.* New York: IEEE, 1974.
[15] L. F. Wei, "Coded M-DPSK with built-in time diversity for fading channels," *IEEE Trans. Inform. Theory*, vol. 39, pp. 1820–1839, Nov. 1993.

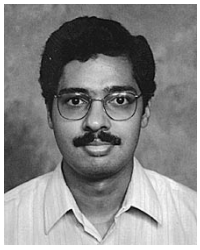

Krishna Balachandran (S'93–M'96) received the B.E. (Hons.) degree in electrical and electronics engineering from Birla Institute of Technology and Science, Pilani, India, in 1992, the M.S. degree in computer and systems engineering, the M.S. degree in mathematics, and the Ph.D. degree in computer and systems engineering from Rensselaer Polytechnic Institute (RPI), Troy, NY, in 1994, 1995, and 1996, respectively.

He has held graduate teaching and research assistantship positions at RPI from 1993 to 1996 and was recognized as a Master Teaching Fellow by the dean of the graduate school, RPI, in 1995. He spent the summers of 1993 and 1994 at Pacific Communication Sciences, Inc., San Diego, CA, where he worked on equalization problems related to digital cellular radio. Since 1996, he has been a Member of Technical Staff in the Performance Analysis Department at Bell Laboratories, Lucent Technologies, Holmdel, NJ, where he has been working on algorithm development, protocol design, and performance analysis for cellular systems. He has published several papers and contributed significantly to evolving cellular standards.

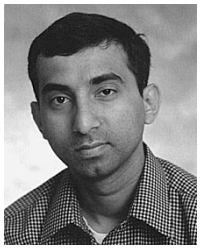

Srinivas R. Kadaba (S'93–M'96) received the B.Tech. degree in electronics and communications engineering from JNT University, Hyderabad, India, in 1989, the M.Sc. (Engg.) degree in electrical communications engineering from the Indian Institute of Science, Bangalore, India, in 1991, and the Ph.D. degree in electrical engineering from Purdue University, West Lafayette, IN, in 1996.

Since July 1996, he has been with the Wireless Core Technology Department, Lucent Technologies, Whippany, NJ, where he is engaged in the analysis and design of wireless communication systems. He has worked on sensor array processing, adaptive algorithms for image processing and wireless communications, and error control coding for voice and data transmission for cellular systems. His current research interests are in resource allocation problems for wireless data networks.

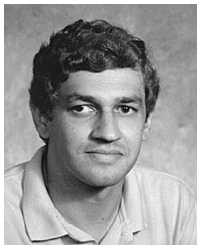

Sanjiv Nanda (S'85–M'88) received the B.Tech. degree in electrical engineering from the Indian Institute of Technology, Kanpur, India, in 1983 and the M.S. degree in mathematics in 1986, and the M.S. and Ph.D. degrees in electrical engineering in 1985 and 1988, respectively, all from the Rensselaer Polytechnic Institute, Troy, NY.

During 1989–1990 he was with the Wireless Information Network Laboratory (WINLAB) at Rutgers University, Piscataway, NJ. Since 1990, he has been with the Performance Analysis Department at Bell Labs, Lucent Technologies, Holmdel, NJ, where he is currently Technical Manager. At Lucent, he has worked on many aspects of cellular system design, including system architecture, protocol design, system performance and link performance. He has published several papers and holds eight U.S. patents. He co-authored a paper on AAL-2 that was chosen as the best paper in Networking in the *Bell Labs Technical Journal* in 1997.

Dr. Nanda's paper on PRMA with D. Goodman and U. Timor won the Jack Neubauer Award of the IEEE Vehicular Technology Society for the best systems paper published in the IEEE TRANSACTIONS ON VEHICULAR TECHNOLOGY in 1991.